



RESEARCH ARTICLE

10.1002/2014JA020808

Special Section:

New perspectives on Earth's radiation belt regions from the prime mission of the Van Allen Probes

Key Points:

- EMFISIS chorus wave intensities are compared to values calculated using the CPDR
- For high wave activity, the CPDR yields underestimates of the wave intensity
- Improved empirical wave models based on direct observations are highly desirable

Correspondence to:

D. P. Hartley,
d.hartley1@lancaster.ac.uk

Citation:

Hartley, D. P., Y. Chen, C. A. Kletzing, M. H. Denton, and W. S. Kurth (2015), Applying the cold plasma dispersion relation to whistler mode chorus waves: EMFISIS wave measurements from the Van Allen Probes, *J. Geophys. Res. Space Physics*, 120, doi:10.1002/2014JA020808.

Received 10 NOV 2014

Accepted 20 JAN 2015

Accepted article online 26 JAN 2015

This is an open access article under the terms of the Creative Commons Attribution License, which permits use, distribution and reproduction in any medium, provided the original work is properly cited.

Applying the cold plasma dispersion relation to whistler mode chorus waves: EMFISIS wave measurements from the Van Allen Probes

D. P. Hartley¹, Y. Chen², C. A. Kletzing³, M. H. Denton⁴, and W. S. Kurth³

¹Physics Department, Lancaster University, Lancaster, UK, ²Los Alamos National Laboratory, Los Alamos, New Mexico, USA, ³Department of Physics and Astronomy, University of Iowa, Iowa City, Iowa, USA, ⁴Space Science Institute, Boulder, Colorado, USA

Abstract Most theoretical wave models require the power in the wave magnetic field in order to determine the effect of chorus waves on radiation belt electrons. However, researchers typically use the cold plasma dispersion relation to approximate the magnetic wave power when only electric field data are available. In this study, the validity of using the cold plasma dispersion relation in this context is tested using Electric and Magnetic Field Instrument Suite and Integrated Science (EMFISIS) observations of both the electric and magnetic spectral intensities in the chorus wave band (0.1–0.9 f_{ce}). Results from this study indicate that the calculated wave intensity is least accurate during periods of enhanced wave activity. For observed wave intensities $>10^{-3}$ nT², using the cold plasma dispersion relation results in an underestimate of the wave intensity by a factor of 2 or greater 56% of the time over the full chorus wave band, 60% of the time for lower band chorus, and 59% of the time for upper band chorus. Hence, during active periods, empirical chorus wave models that are reliant on the cold plasma dispersion relation will underestimate chorus wave intensities to a significant degree, thus causing questionable calculation of wave-particle resonance effects on MeV electrons.

1. Introduction

Relativistic electron fluxes in the outer radiation belt ($3 < L < 7$) are highly dynamic during periods with enhanced geomagnetic activity [e.g., *Onsager et al.*, 2002; *Green et al.*, 2004; *Borovsky and Denton*, 2009; *Hartley et al.*, 2014]. This variability is driven by an imbalance between source, loss, and transport mechanisms, each of which may become enhanced during geomagnetic storms [e.g., *Reeves et al.*, 2003; *Chen et al.*, 2007a; *Liemohn and Chan*, 2007; *Morley et al.*, 2010; *Turner et al.*, 2012; *Hartley et al.*, 2013].

Previous studies indicate that enhancements of energetic electrons in the outer radiation belt are driven by acceleration processes within the magnetosphere [e.g., *Li et al.*, 1997]. It is well established that radial diffusion, which violates the third adiabatic invariant of particle motion, can transport electrons inward and therefore increase their energy through betatron and Fermi acceleration processes [e.g., *Schulz and Lanzerotti*, 1974]. This type of acceleration requires positive gradients in the phase space density versus L shell profile inward of the source region. Recent studies have shown that persistent local maxima in the phase space density profiles exist between $L = 4$ and $L = 5.5$ [e.g., *Green and Kivelson*, 2004; *Chen et al.*, 2007b; *Turner et al.*, 2010; *Shprits et al.*, 2012; *Reeves et al.*, 2013]. These studies demonstrate that local acceleration mechanisms, such as wave-particle interactions, which violate the first and second adiabatic invariants of particle motion, are also at work within the outer belt region.

Whistler mode chorus waves are considered to be highly efficient for local acceleration of electrons up to relativistic energies [*Summers et al.*, 1998; *Thorne*, 2010]. Chorus waves are in the VLF range (~ 100 Hz to tens of kilohertz) and typically occur in two bands, lower and upper, typically separated by a gap at half of the electron gyrofrequency. Modeling electron resonances with this type of wave requires the knowledge of chorus distributions, a topic that has been actively studied [e.g., *Horne and Thorne*, 2003; *Meredith et al.*, 2003a; *Li et al.*, 2009a, 2009b; *Tu et al.*, 2013]. Aside from the recently developed particle proxies [e.g., *Li et al.*, 2013; *Chen et al.*, 2014], empirical chorus models [e.g., *Meredith et al.*, 2003a, 2012] are traditionally used. However, when no magnetic wave field data were available, previous studies used cold plasma theory to infer the magnetic wave power from electric field observations, and thus, current empirical wave models are based on this assumption. Recently, equipped with comprehensive wave and plasma instruments,

the successfully operating Van Allen Probes mission provides an opportunity to explore the validity of this assumption.

2. Motivation and Methodology

Previous studies often used the wave data set from the Combined Release and Radiation Effects Satellite (CRRES) to examine the role of chorus waves in radiation belt dynamics, more specifically, the acceleration of electrons to MeV energies [e.g., Meredith *et al.*, 2003a, 2003b, 2012]. The Plasma Wave Experiment (PWE) on board the CRRES satellite measured wave electric fields with high resolution in the frequency range 5.6 Hz to 400 kHz, which fully covers the chorus frequency range [Anderson and Gurnett, 1992]. Given the need to investigate the energization of radiation belt electrons, and given that energy diffusion rates scale with the magnetic field intensity [Kennel and Engelmann, 1966; Summers and Ma, 2000], it was necessary to convert the electric field spectral intensities (as measured by CRRES) to magnetic field spectral intensities. This can be performed using the expression

$$S_B = \frac{1}{c^2} \left(1 - \frac{f_{pe}^2}{f(f - f_{ce})} \right) S_E \quad (1)$$

which is derived from Maxwell's third equation (Faraday's law), assuming a cold plasma dispersion relation for parallel-propagating whistler mode waves [Meredith *et al.*, 2004]. Here S_B and S_E are the magnetic and electric field spectral intensities, respectively, c is the speed of light, f is the wave frequency, f_{pe} is the electron plasma frequency, and f_{ce} is the electron gyrofrequency. The applicability of the cold plasma dispersion relation in this manner was untested when employed in previous studies. Of course the cold plasma dispersion relation is applicable in a cold plasma; however, when the plasma has a significant warm/hot component, implementation of the cold plasma dispersion relation may result in large uncertainties of calculated quantities. For example, the cold plasma dispersion relation is likely to yield accurate results when applied to hiss [e.g., Meredith *et al.*, 2004] inside of the plasmasphere (a relatively cold magnetospheric plasma ~ 1 eV). Outside of the plasmasphere the plasma is warmer and thus the cold plasma dispersion relation may not be as applicable to chorus waves that occur in this region [e.g., Meredith *et al.*, 2003a].

With the comprehensive wave instrumentation now available aboard the Van Allen Probes mission, it is possible to test the accuracy of using the cold plasma dispersion relation to calculate the integral magnetic field intensity. The Waves Instrument, part of the Electric and Magnetic Field Instrument Suite and Integrated Science (EMFISIS) instrument suite, on board the Van Allen Probes [Kletzing *et al.*, 2013] measures both electric and magnetic field spectral intensities across the chorus wave frequency range. Comparing the measured magnetic field spectral intensity with the calculated magnetic field spectral intensity (using the measured electric field spectral intensity and equation (1)) provides a quantitative determination of the accuracy of the cold plasma assumption. The electron gyrofrequency is easily calculated using the magnetic field measured by the Van Allen Probes EMFISIS magnetometer instrument, while the plasma frequency, f_{pe} , is inferred from the upper hybrid line (UHL). The plasma frequency data set inferred from the UHL is not yet complete and therefore only available for those orbits processed to date.

Using the measured electric field spectral intensity and equation (1), the magnetic field spectral intensity is calculated [e.g., Meredith *et al.*, 2003a, 2003b, 2004, 2012]. This quantity is then integrated across the full (0.1–0.9 f_{ce}), lower (0.1–0.5 f_{ce}), and upper (0.5–0.9 f_{ce}) band chorus frequency ranges in order to calculate the chorus wave intensities. These calculated wave intensities can then be directly compared to the observed chorus wave intensities as a test of the cold plasma assumption.

Plasmaspheric hiss can also occur in the lower band chorus frequency range at low L shells (inside the plasmasphere). Therefore, in this study, the plasma density is required to be less than $10 \times (6.6/L)^4$ or 30 cm^{-3} (whichever is smaller) in order for a location to be defined as outside of the plasmasphere, thus excluding plasmaspheric hiss emissions [e.g., Li *et al.*, 2014].

The method described above is applied to a 20 day sample of Van Allen Probe A data where the plasma frequency, f_{pe} , inferred from the UHL, is available. This data sample provides preliminary results that span a limited range of L shells, MLT, solar wind conditions, and geomagnetic activity indices. However, during this sample period, a broad range of wave activity levels are observed, thus allowing for the accuracy of using

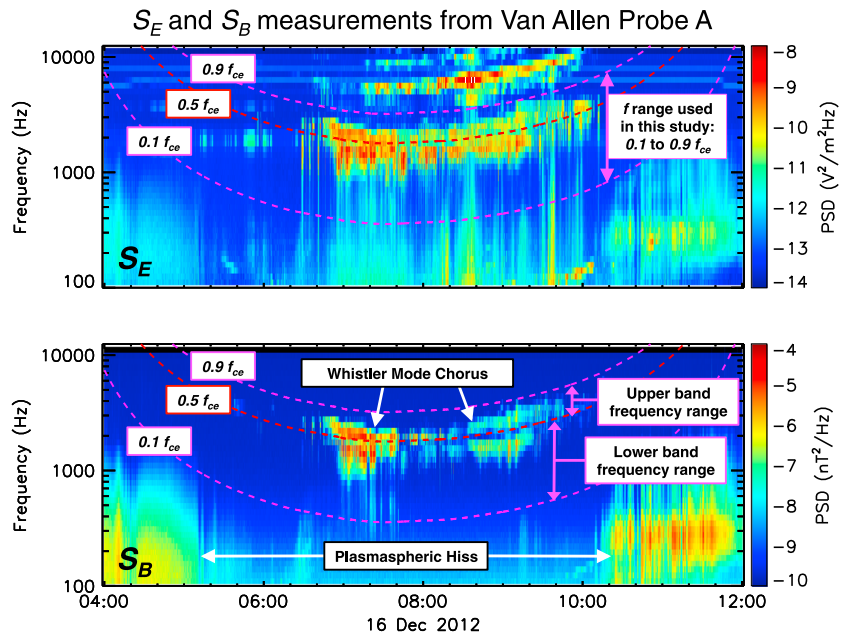


Figure 1. A survey plot of the (top) electric, S_E , and (bottom) magnetic, S_B , wave spectral intensity observed by Van Allen Probe A during an 8 h period on 16 December 2012. The dashed pink lines indicate $0.1 f_{ce}$ and $0.9 f_{ce}$, and the dashed red line indicates $0.5 f_{ce}$ as calculated from the onboard magnetometer measurements. Whistler mode chorus waves and plasmaspheric hiss are highlighted in the spectrogram.

the cold plasma dispersion relation to calculate the magnetic field spectral intensity, and wave intensity, to be tested across a range of conditions. For data quality, two of the measured frequency bands (centered around ~ 2 and 4 kHz) are removed due to increased noise levels. Since the same frequency bands are removed from both the electric and magnetic field wave observations, the calculated integral wave powers remain comparable. Also, in this study, the instrument background levels are subtracted from both the electric and magnetic field spectral intensities. If the background subtraction results in either electric or magnetic spectral intensities below 0 at a given frequency, the spectral intensity of both the wave electric and magnetic fields is set to 0 at this frequency.

3. Results

First, the measured spectral intensity of the electric and magnetic wave field is observed for a sample case where whistler mode chorus waves are present. Figure 1 shows the electric, S_E (top), and magnetic, S_B (bottom), wave spectral intensities observed by Van Allen Probe A during an 8 h period on 16 December 2012. The dashed pink lines indicate $0.1 f_{ce}$ and $0.9 f_{ce}$, and the dashed red line indicates $0.5 f_{ce}$ as calculated from the onboard magnetometer measurements. Whistler mode chorus waves are evident in both the electric and magnetic fields spectral intensity, occurring in two bands, lower and upper, separated by half of the electron gyrofrequency. Plasmaspheric hiss is also evident—an unstructured emission that is generally confined to the plasmasphere occurring at frequencies below a few thousand hertz.

As a test of the methodology described above, the measured power spectral density is compared to that calculated using the cold plasma dispersion relation. Figure 2 displays the power spectral density of the wave magnetic field in the chorus wave frequency range as measured by EMFISIS (blue) and as calculated using the cold plasma dispersion relation (red) for three instances of time. The normalized root-mean-square (RMS) deviations are also listed. For the first time instance, 12:01:41 on 20 November 2012 (Figure 2a), using the cold plasma dispersion relation allows for the magnetic field power spectral density between 0.1 and $0.9 f_{ce}$ to be accurately calculated. That is, the red and blue lines shown in Figure 2a match extremely well. Both upper and lower band chorus waves are apparent during this period with a gap between the two at approximately half of the electron gyrofrequency. The normalized RMS error is very low for this time instance (0.111). For the second instance of time, 11:21:47 on 20 November 2012 (Figure 2b), using the cold plasma dispersion relation results in the calculated power spectral density being around 1 order of

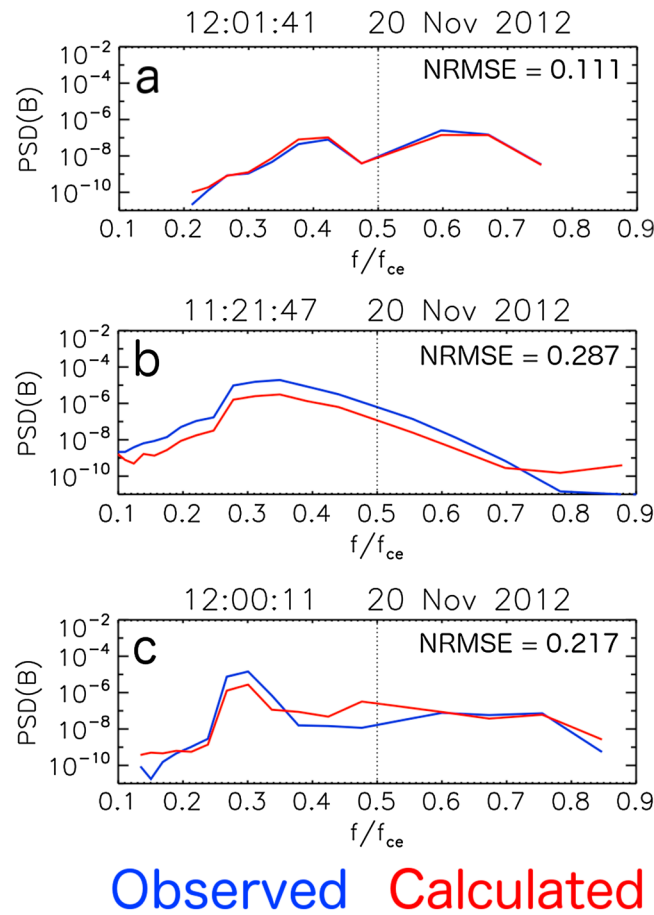


Figure 2. The magnetic field power spectral density in the chorus wave frequency band (between 0.1 and 0.9 f_{ce}) as measured by EMFISIS on board Van Allen Probe A (blue) and as calculated using the cold plasma dispersion relation (red) at (a) 12:01:41, (b) 11:21:47, and (c) 12:00:11 on 20 November 2012. The normalized root-mean-square errors (NRMSE) are also listed.

magnitude less than that observed across the entire lower band chorus wave frequency range. That is, the red line in Figure 2b is significantly lower than the blue line over the entire 0.1–0.5 f_{ce} frequency range. The normalized RMS error for this time instance is 0.287. For the third time instance, 12:00:11 on 20 November 2012 (Figure 2c), the shape of the calculated power spectral density does not quite match that observed by EMFISIS. That is, in contrast to the systematic shift in power spectral density shown in Figure 2b, the discrepancies in this case are frequency dependent. At some frequencies the calculated power spectral density is greater than that observed, and at other frequencies the calculated power spectral density is less than that observed. The normalized RMS error for this time instance is 0.217. Discrepancies between the observed and calculated quantities, such as those shown in Figures 2b and 2c, will certainly affect the calculated integral magnetic field wave intensity, B_w^2 . Cases similar to those shown in Figure 2b (systematic shift) will result in significant errors in the calculated chorus wave intensity. Cases similar to those shown in Figure 2c (frequency-dependent error) may result in errors in the calculated chorus wave intensity; however, it is also

possible that when integrated to calculate the wave intensity in the chorus frequency range, the discrepancies could cancel out resulting in the calculated wave intensity matching that measured by the Van Allen Probes. Despite the normalized RMS errors shown in Figures 2b and 2c being approximately equal, in cases similar to that shown in Figure 2c it is likely that the calculated integral wave intensity will be less affected by these deviations in comparison to cases similar to that presented in Figure 2b.

Applying the methodology described in section 2 to a 20 day sample of Van Allen Probe A EMFISIS wave data where the plasma frequency inferred from the UHL is available allows for the accuracy of using the cold plasma dispersion relation to be considered. Figure 3a compares measured and calculated magnetic field chorus wave intensity, the integral of the power spectral density between 0.1 and 0.9 f_{ce} . The color indicates the number of occurrences in each bin, normalized to the maximum event number in each observed wave intensity column. In this way, distributions of calculated magnetic wave intensities for a given observed magnetic wave intensity can be clearly seen. If all calculated wave intensities were equal to those observed (i.e., the cold plasma assumption yielded perfect results), all points would lie on the diagonal equivalence line. Also shown are the number of occurrences in each observed wave intensity column, in addition to the total number of occurrences (ΣN) and the number of occurrences with high observed wave intensity ($\Sigma N (B_w^2 > 10^{-3} nT^2)$). It is apparent that for the vast majority of the period studied, the calculated magnetic field wave intensity is relatively close to that observed by Van Allen Probe A. During periods of low observed magnetic field wave intensity, there are a number of points that lie above the line of equivalence, with some calculated values greater than 3 orders of magnitude larger than those observed. At times when the

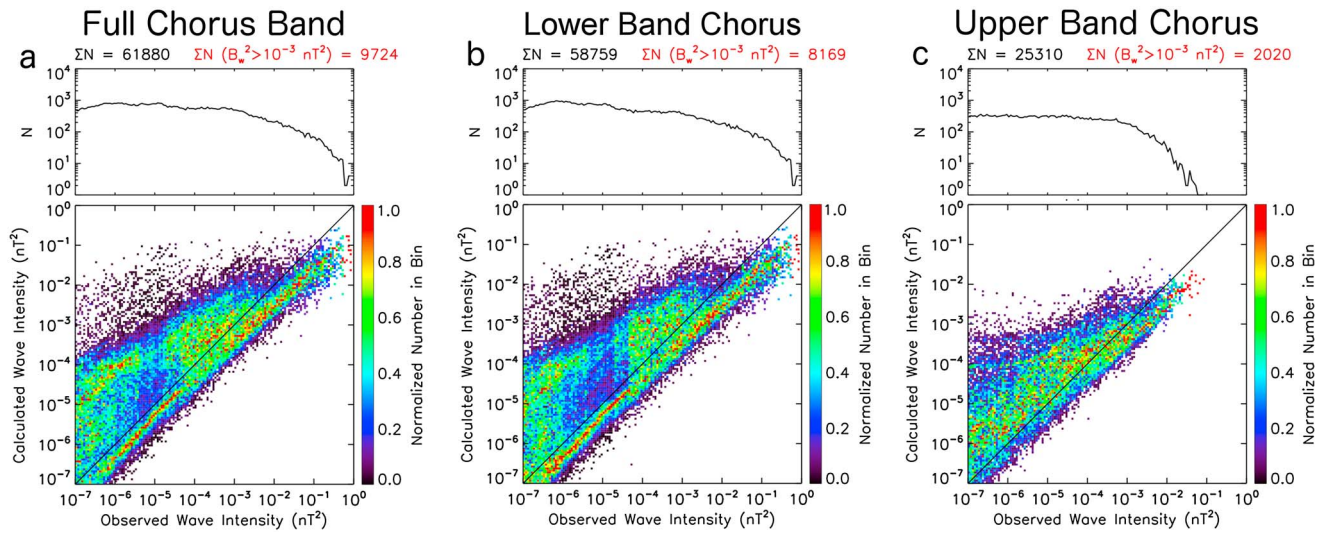


Figure 3. (a) Plot showing how the observed wave intensity from Van Allen Probe A compares with that calculated using the cold plasma dispersion relation in the 0.1 to $0.9 f_{ce}$ range for the 20 day sample period used in this study. The color indicates the number of occurrences in each bin, normalized to the number of occurrences in each observed wave intensity column. The line plot above each panel indicates the number of occurrences in each observed wave intensity column, in addition to listing the total number of occurrences (ΣN) and the number of occurrences with high observed wave intensity ($\Sigma N (B_w^2 > 10^{-3} nT^2)$). The same quantities calculated separately for (b) lower band (0.1 to $0.5 f_{ce}$) and (c) upper band (0.5 to $0.9 f_{ce}$) chorus frequencies.

observed magnetic field wave intensity is elevated ($B_w^2 > 10^{-3} nT^2$), the higher density of points appears to drift below the line of equivalence; the observed magnetic field wave intensity is greater than that calculated using the cold plasma dispersion relation.

To further investigate whether using the cold plasma dispersion relation to calculate magnetic field power spectral densities, and thus wave intensities, is more accurate for specific frequency bands, the data are sorted between lower (0.1 and $0.5 f_{ce}$) and upper (0.5 and $0.9 f_{ce}$) band chorus frequencies. Figures 3b and 3c display the same quantities as shown in Figure 3a after this sorting in frequency band has taken place. It is apparent that wave intensities are generally higher in the lower band chorus frequency range compared to those in the upper band chorus frequency range. The structure observed for lower band chorus wave frequencies (Figure 3b) is largely similar to that observed for the full chorus band (Figure 3a). Again, during periods of low observed magnetic field wave intensity, there are a number of points significantly above the line of equivalence with some calculated quantities over 3 orders of magnitude larger than those observed. At times when the observed magnetic field wave intensity is elevated ($B_w^2 > 10^{-3} nT^2$), the higher density of points exists below the equivalence line with very few data points above the equivalence line. That is, the observed magnetic field wave intensity is generally greater than that calculated using the cold plasma dispersion relation during elevated chorus activity. For upper band chorus frequencies (Figure 3c), there is a substantially greater spread of data from the line of equivalence than for lower band chorus frequencies. Thus, using the cold plasma dispersion relation to calculate upper band chorus wave intensity will result in a greater number of deviations from the observed magnetic wave intensity when compared to the same technique used for lower band chorus frequencies.

In order to better understand the deviations from the line of equivalence, the ratio of calculated and observed wave intensities (observed/calculated) is considered for both low and elevated wave activities. Low wave intensity is parametrized as $B_w^2 < 10^{-3} nT^2$ and elevated wave intensity as $B_w^2 > 10^{-3} nT^2$. Figures 4a and 4b show the probability distributions of the logarithm of the wave intensity ratio in the full chorus wave frequency band (observed/calculated) for both low and elevated observed wave intensities, respectively. Also shown are the percentages of data that occur in discreet ratio bins parametrized as calculated wave intensity is an overestimate by greater than a factor of 5 (Ratio < 0.2 , dark blue), calculated wave intensity is an overestimate by greater than a factor of 2 but by less than a factor of 5 ($0.2 < \text{Ratio} < 0.5$, light blue), calculated wave intensity is within a factor of 2 of the observed value ($0.5 < \text{Ratio} < 2.0$, green), calculated wave intensity is an underestimate by greater than a factor of 2 but by less than a factor of 5 ($2.0 < \text{Ratio} < 5.0$, orange), and calculated wave intensity is an underestimate by greater than a factor of 5

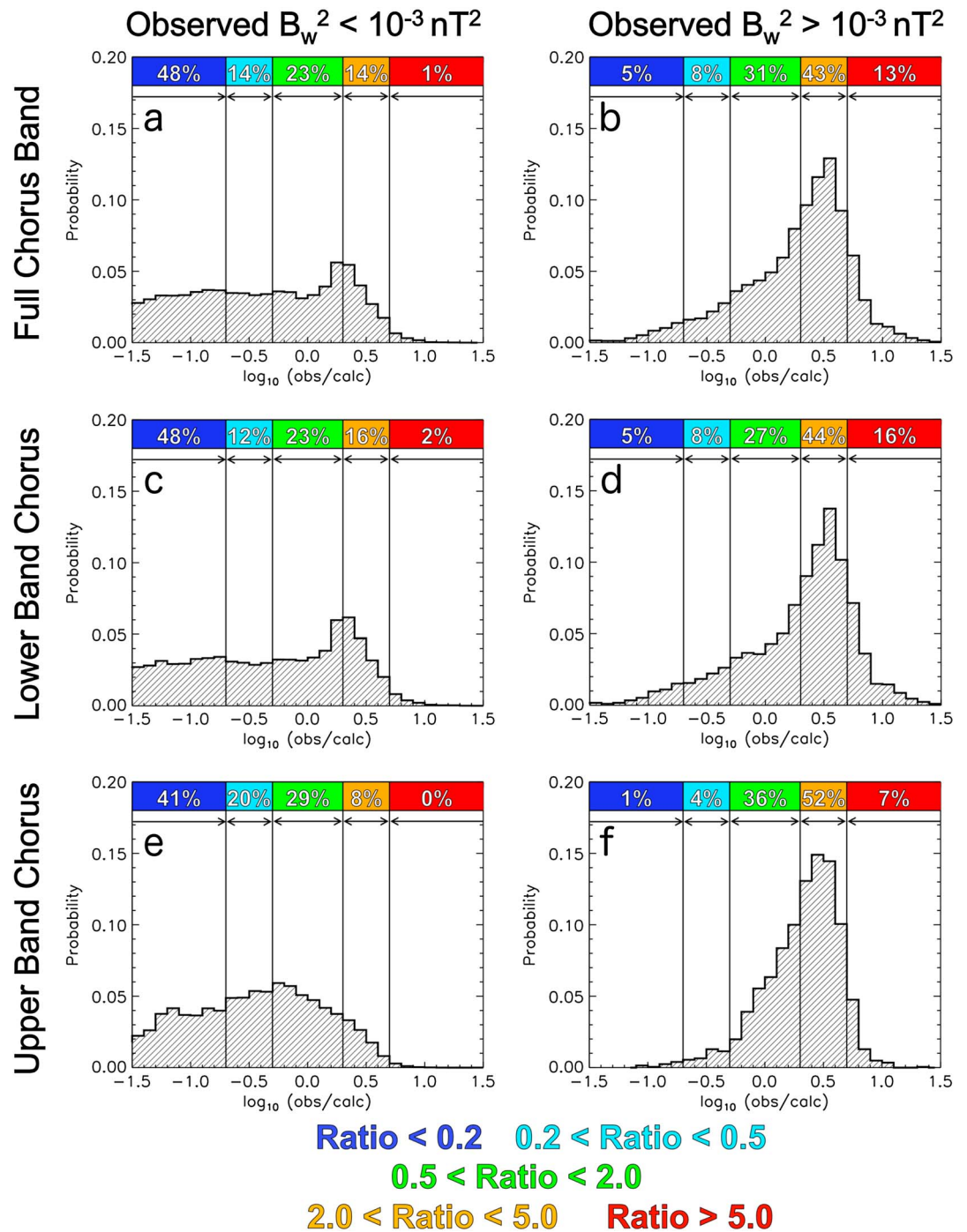


Figure 4. The probability distributions of the logarithm of the wave intensity ratio (observed/calculated) in the full chorus wave frequency band for (a) low ($B_w^2 < 10^{-3} \text{ nT}^2$) and (b) elevated ($B_w^2 > 10^{-3} \text{ nT}^2$) observed wave intensities. Also shown are the percentages of data that occur in discreet ratio bins parametrized as Ratio < 0.2, 0.2 < Ratio < 0.5, 0.5 < Ratio < 2.0, 2.0 < Ratio < 5.0, and Ratio > 5.0. The same parameters for (c, d) lower band chorus and (e, f) upper band chorus.

(Ratio > 5.0, red). For the full chorus band, the mean wave intensity ratio is 0.83 (−0.08 on logarithmic scale) during low wave activity. That is, on average using the cold plasma dispersion relation to calculate the wave intensity between 0.1 and 0.9 f_{ce} will yield relatively accurate results during low wave activity. However, during elevated chorus activity, the mean wave intensity ratio is 2.88 (0.46 on logarithmic axis). Therefore, on average, using the cold plasma dispersion relation will result in an underestimate of the wave intensity

by a factor of ~ 3 during periods of intense wave activity. There is a clear shift in the distribution toward underestimates of the calculated wave intensity when considering only periods of enhanced wave activity. The percentages listed in Figures 4a and 4b reveal that for elevated observed wave activity ($B_w^2 > 10^{-3} \text{ nT}^2$), the calculated wave intensity is an underestimate by a factor of 2 or greater for 56% of the data (sum of percentages where $2.0 < \text{Ratio} < 5.0$ and $\text{Ratio} > 5.0$).

The probability distributions for lower band chorus wave frequencies, as shown in Figures 4c and 4d, exhibit similar structure to that observed for the full chorus band. The mean wave intensity ratio is 0.92 (-0.04 on logarithmic scale) during low wave activity (Figure 4c). This again implies that, on average, using the cold plasma dispersion relation to calculate lower band chorus wave intensities will yield relatively accurate results during low wave activity. However, during enhanced chorus activity (Figure 4d) the mean wave intensity ratio is 3.15 (0.50 on logarithmic axis). This means that on average, using the cold plasma dispersion relation to calculate lower band chorus wave intensities will result in an underestimate by a factor of ~ 3 during periods of elevated chorus wave activity. The probability distributions for upper band chorus are shown in Figures 4e and 4f. Again, during elevated wave activity (Figure 4f), the average upper band chorus wave intensity ratio is greater than unity (2.59, 0.42 on logarithmic scale). This implies that on average, using the cold plasma dispersion relation to calculate the upper band chorus wave intensity will result in an underestimate by a factor of ~ 2.5 during active periods.

4. Discussion

This study addresses the applicability of using the cold plasma dispersion relation to calculate magnetic field spectral intensities, S_B , from electric field spectral intensities, S_E , in a plasma that may contain a significant warm/hot component [cf. Meredith *et al.*, 2003a, 2003b, 2004, 2012].

Results indicate that on average, wave intensities calculated using the cold plasma dispersion relation closely match observations during periods of low activity. However, during elevated wave activity ($B_w^2 > 10^{-3} \text{ nT}^2$), there is a clear shift in the distributions which clearly indicates that using the cold plasma dispersion relation will result in underestimates of the chorus wave intensity. That is, using the cold plasma dispersion relation to calculate the chorus wave intensity results, on average, in an underestimate by a factor of ~ 3 for the full band, ~ 3 for lower band, and ~ 2.5 for upper band on average during enhanced wave activity. For lower band chorus waves, using the cold plasma dispersion relation to calculate the wave intensity results in an underestimate by a factor of 2, or greater, 60% of the time. For waves in the upper chorus frequency band, this number is 59%, although the number of larger underestimates is significantly lower. These discrepancy percentages, particularly for lower band chorus waves, highlight the need for new empirical wave models based on direct observations.

Some possible explanations for the discrepancies that arise from implementing the cold plasma dispersion relation are considered. First, implementation of the cold plasma dispersion relation in a plasma that has a significant warm/hot component may explain the observed deviations of ratios away from unity. Second, large-amplitude chorus waves may propagate highly obliquely in a quasi-electrostatic mode [e.g., Agapitov *et al.*, 2013]. Given that the wave propagation angle is not identified in this study, this may be a factor that contributes toward the observed discrepancies in calculated wave intensity. The uncertainty in the inferred plasma frequency is between 10 and 20%, which would lead to a maximum error factor of ~ 1.44 in the spectral intensities. Hence, errors in the determined f_{pe} cannot fully explain the observed factor of 2 or greater deviations.

5. Conclusions

In this study, EMFISIS observations of chorus wave magnetic spectral intensities have been directly compared to spectral intensities calculated using the cold plasma dispersion relation and the wave electric field. The direct comparison between observed and calculated wave intensities reveals that for observed wave intensities $> 10^{-3} \text{ nT}^2$, using the cold plasma dispersion relation results in an underestimate of the wave intensity by a factor of 2 or greater 56% of the time over the full chorus wave band, 60% of the time for lower band chorus, and 59% of the time for upper band chorus. The impact of this is that empirical wave models that are based on CRRES data may tend to underestimate the chorus wave intensity during active periods, and thus wave-particle resonance effects (i.e., energy diffusion rates which scale with the magnetic field

wave intensity [Kennel and Engelmann, 1966; Summers and Ma, 2000]) on MeV electrons may be underestimated. Therefore, improved empirical wave models based upon direct measurements from the Van Allen Probes are highly desirable.

Acknowledgments

Research at Lancaster is supported by a Science and Technology Facilities Council (STFC) studentship grant. Part of this work was carried out during the 2013 Los Alamos Space Weather Summer School and funded by NSF National Space Weather Program (project 1131871). D.P. Hartley would like to thank the Los Alamos Space Weather Summer School, Royal Astronomical Society Conference Travel Fund, the Institute of Physics Research Student Conference Fund, and the C R Barber Trust for financial support. Yue Chen is funded by RBSP funding contract NNG13PJ051. Part of this work was performed under support of JHU/APL contract 921647 under NASA Prime contract NAS5-01072. Van Allen Probes EMFISIS data are available at <http://emfisis.physics.uiowa.edu/data/index>.

Michael Balikhin thanks James McCollough and another reviewer for their assistance in evaluating this paper.

References

- Agapitov, O., A. Artemyev, V. Krasnoselskikh, Y. V. Khotyaintsev, D. Mourenas, H. Breuillard, M. Balikhin, and G. Rolland (2013), Statistics of whistler mode waves in the outer radiation belt: Cluster STAFF-SA measurements, *J. Geophys. Res. Space Physics*, *118*, 3407–3420, doi:10.1002/jgra.50312.
- Anderson, R. R., and D. A. Gurnett (1992), The development of static and dynamic models of the Earth's radiation belt environment through the study of plasma waves, wave-particle interactions and plasma number densities from in situ observations in the Earth's magnetosphere with the CRRES SPACERAD instruments, *PL-TR-92-2035*, Philips Lab., Hanscom AFB, Mass.
- Borovsky, J. E., and M. H. Denton (2009), Relativistic-electron dropouts and recovery: A superposed epoch study of the magnetosphere and the solar wind, *J. Geophys. Res.*, *114*, A02201, doi:10.1029/2008JA013128.
- Chen, Y., R. H. W. Friedel, G. D. Reeves, T. E. Cayton, and R. Christensen (2007a), Multisatellite determination of the relativistic electron phase space density at geosynchronous orbit: An integrated investigation during geomagnetic storm times, *J. Geophys. Res.*, *112*, A11214, doi:10.1029/2007JA012314.
- Chen, Y., G. D. Reeves, and R. H. Friedel (2007b), The energization of relativistic electrons in the outer Van Allen radiation belt, *Nat. Phys.*, *3*, 614–617, doi:10.1038/nphys655.
- Chen, Y., G. D. Reeves, R. H. Friedel, and G. S. Cunningham (2014), Global time-dependent chorus maps from low-Earth-orbit electron precipitation and Van Allen Probes data, *Geophys. Res. Lett.*, *41*, 755–761, doi:10.1002/2013GL059181.
- Green, J. C., and M. G. Kivelson (2004), Relativistic electrons in the outer radiation belt: Differentiating between acceleration mechanisms, *J. Geophys. Res.*, *109*, A03213, doi:10.1029/2003JA010153.
- Green, J. C., T. G. Onsager, T. P. O'Brien, and D. N. Baker (2004), Testing loss mechanisms capable of rapidly depleting relativistic electron flux in the Earth's outer radiation belt, *J. Geophys. Res.*, *109*, A12211, doi:10.1029/2004JA010579.
- Hartley, D. P., M. H. Denton, J. C. Green, T. G. Onsager, J. V. Rodriguez, and H. J. Singer (2013), Case studies of the impact of high-speed solar wind streams on the electron radiation belt at geosynchronous orbit: Flux, magnetic field, and phase space density, *J. Geophys. Res. Space Physics*, *118*, 6964–6979, doi:10.1002/2013JA018923.
- Hartley, D. P., M. H. Denton, and J. V. Rodriguez (2014), Electron number density, temperature, and energy density at GEO and links to the solar wind: A simple predictive capability, *J. Geophys. Res. Space Physics*, *119*, 4556–4571, doi:10.1002/2014JA019779.
- Horne, R. B., and R. M. Thorne (2003), Relativistic electron acceleration and precipitation during resonant interactions with whistler-mode chorus, *Geophys. Res. Lett.*, *30*(10), 1527, doi:10.1029/2003GL016973.
- Kennel, C. F., and F. Engelmann (1966), Velocity space diffusion from weak plasma turbulence in a magnetic field, *Phys. Fluids*, *9*, 2377–2388, doi:10.1063/1.1761629.
- Kletzing, C. A., et al. (2013), The Electric and Magnetic Field Instrument Suite and Integrated Science (EMFISIS) on RBSP, *Space Sci. Rev.*, *179*, 127–181, doi:10.1007/s11214-013-9993-6.
- Li, X., D. N. Baker, M. Temerin, D. Larson, R. P. Lin, G. D. Reeves, M. Looper, S. G. Kanekal, and R. A. Mewaldt (1997), Are energetic electrons in the solar wind the source of the outer radiation belt?, *Geophys. Res. Lett.*, *24*(8), 923–926.
- Li, W., R. M. Thorne, V. Angelopoulos, J. Bortnik, C. M. Cully, B. Ni, O. LeContel, A. Roux, U. Auster, and W. Magnes (2009a), Global distribution of whistler-mode chorus waves observed on the THEMIS spacecraft, *Geophys. Res. Lett.*, *36*, L09104, doi:10.1029/2009GL037595.
- Li, W., R. M. Thorne, V. Angelopoulos, J. W. Bonnell, J. P. McFadden, C. W. Carlson, O. LeContel, A. Roux, K. H. Glassmeier, and H. U. Auster (2009b), Evaluation of whistler-mode chorus intensification on the nightside during an injection event observed on the THEMIS spacecraft, *J. Geophys. Res.*, *114*, A00C14, doi:10.1029/2008JA013554.
- Li, W., B. Ni, R. M. Thorne, J. Bortnik, J. C. Green, C. A. Kletzing, W. S. Kurth, and G. B. Hospodarsky (2013), Constructing the global distribution of chorus wave intensity using measurements of electrons by the POES satellites and waves by the Van Allen Probes, *Geophys. Res. Lett.*, *40*, 4526–4532, doi:10.1002/grl.50920.
- Li, W., et al. (2014), Evidence of stronger pitch angle scattering loss caused by oblique whistler-mode waves as compared with quasi-parallel waves, *Geophys. Res. Lett.*, *41*, 6063–6070, doi:10.1002/2014GL061260.
- Liemohn, M. W., and A. A. Chan (2007), Unravelling the causes of radiation belt enhancements, *Eos Trans. AGU*, *88*(42), 425–426, doi:10.1029/2007EO420001.
- Meredith, N. P., R. B. Horne, R. M. Thorne, and R. R. Anderson (2003a), Favored regions for chorus-driven electron acceleration to relativistic energies in the Earth's outer radiation belt, *Geophys. Res. Lett.*, *30*(16), 1871, doi:10.1029/2003GL017698.
- Meredith, N. P., M. Cain, R. B. Horne, R. M. Thorne, D. Summers, and R. R. Anderson (2003b), Evidence for chorus-driven electron acceleration to relativistic energies from a survey of geomagnetically disturbed periods, *J. Geophys. Res.*, *108*(A6), 1248, doi:10.1029/2002JA009764.
- Meredith, N. P., R. B. Horne, R. M. Thorne, D. Summers, and R. R. Anderson (2004), Substorm dependence of plasmaspheric hiss, *J. Geophys. Res.*, *109*, A06209, doi:10.1029/2004JA010387.
- Meredith, N. P., R. B. Thorne, A. Sicard-Piet, D. Boscher, K. H. Yearby, W. Li, and R. M. Thorne (2012), Global model of lower band and upper band chorus from multiple satellite observations, *J. Geophys. Res.*, *117*, A10225, doi:10.1029/2012JA017978.
- Morley, S. K., R. H. W. Friedel, E. L. Spanswick, G. D. Reeves, J. T. Steinberg, J. Koller, T. Cayton, and E. Noveroske (2010), Dropouts of the outer electron radiation belt in response to solar wind stream interfaces: Global positioning system observations, *Proc. R. Soc. A*, *466*, 3329–3350, doi:10.1098/rspa.2010.0078, first published online 6 May 2010.
- Onsager, T. G., G. Rostoker, H.-J. Kim, G. D. Reeves, T. Obara, H. J. Singer, and C. Smithro (2002), Radiation belt electron flux dropouts: Local time, radial, and particle-energy dependence, *J. Geophys. Res.*, *107*(A11), 1382, doi:10.1029/2001JA000187.
- Reeves, G. D., K. L. McAdams, R. H. W. Friedel, and T. P. O'Brien (2003), Acceleration and loss of relativistic electrons during geomagnetic storms, *Geophys. Res. Lett.*, *30*(10), 1529, doi:10.1029/2002GL016513.
- Reeves, G. D., et al. (2013), Electron acceleration in the heart of the Van Allen radiation belts, *Science*, *341*, 991–994, doi:10.1126/science.1237743.
- Schulz, M., and L. J. Lanzerotti (1974), *Particle Diffusion in the Radiation Belts*, Springer, New York.
- Shprits, Y., M. Daae, and B. Ni (2012), Statistical analysis of phase space density buildups and dropouts, *J. Geophys. Res.*, *117*, A01219, doi:10.1029/2011JA016939.

- Summers, D., and C. Ma (2000), A model for generating relativistic electrons in the Earth's inner magnetosphere based on gyroresonant wave-particle interactions, *J. Geophys. Res.*, *105*(A2), 2625–2639.
- Summers, D., R. M. Thorne, and F. Xiao (1998), Relativistic theory of wave-particle resonant diffusion with application to electron acceleration in the magnetosphere, *J. Geophys. Res.*, *103*(A9), 20,487–20,500, doi:10.1029/98JA01740.
- Thorne, R. M. (2010), Radiation belt dynamics: The importance of wave-particle interactions, *Geophys. Res. Lett.*, *37*, L22107, doi:10.1029/2010GL044990.
- Tu, W., G. S. Cunningham, Y. Chen, M. G. Henderson, E. Camporeale, and G. D. Reeves (2013), Modeling radiation belt electron dynamics during GEM challenge intervals with the DREAM3D diffusion model, *J. Geophys. Res. Space Physics*, *118*, 6197–6211, doi:10.1002/jgra.50560.
- Turner, D. L., X. Li, G. D. Reeves, and H. J. Singer (2010), On phase space density radial gradients of Earth's outer-belt electrons prior to sudden solar wind pressure enhancements: Results from distinctive events and a superposed epoch analysis, *J. Geophys. Res.*, *115*, A01205, doi:10.1029/2009JA014423.
- Turner, D. L., Y. Shprits, M. Hartinger, and V. Angelopoulos (2012), Explaining sudden losses of outer radiation belt electrons during geomagnetic storms, *Nat. Phys.*, *8*, 208–212, doi:10.1038/nphys2185.